Journal of Chemical&Engineering Data

pubs.acs.org/jced

Article

A Geometric Approach for the Calculation of the Nonrandomness Factor Using Computational Chemistry

Pedro Velho,* Leonor R. Barroca, and Eugénia A. Macedo

Cite This: J. Chem. Eng. Data 2024, 69, 3573−3583

Read Online

ACCESS | Metrics & More | Article Recommendations | Supporting Information

ABSTRACT: The nonrandomness factor (α) is a parameter related to the polarity (and consequent randomness of spatial orientation) of the molecules and is generally fixed between 0.20 and 0.47 since no technique has been developed so far for its accurate estimation. However, the consideration of a constant nonrandomness factor for mixtures is known to harden azeotrope description and to cause convergence issues in both the Nonrandom Two-Liquid (NRTL) and Universal Quasi-chemical (UNIQUAC) models, which have been widely applied in the correlation of phase equilibria. In this work, a novel geometric methodology, named Porto's approach, was applied in the calculation of the nonrandomness factors for 50 pure components (mainly alkanes, alcohols, and ketones) at 298.15 K and 0.1 MPa. This methodology relied on computational chemistry (Density Functional Theory, DFT) to minimize the energy of molecules in a cavity within a solvent composed of molecules of their own (applying the Polarizable Continuum Model, PCM), and thereafter define the most stable chemical configuration in the pure liquid state. Then, the nonrandomness factor of each component was determined based on its molecular dipole moment, which was calculated after a population analysis of the optimized partial electrical charges with the Natural Bond Orbital (NBO) function. This innovative approach was applied in the correlation of liquid−liquid equilibria (LLE) data for 15 ternary systems comprising only neutral molecules with NRTL and UNIQUAC. The classical methods (α = 0.2 or 0.3 for NRTL and α = 0.2 for UNIQUAC) were compared against the usage of a component-specific nonrandomness factor, and similar standard deviations were obtained. Hence, this work is considered a strong advance in the application of these excess free Gibbs energy models to phase equilibria estimation and opens the door to more accurate thermodynamic modeling of nonideal mixtures (such as the ones containing electrolytes) by providing enhanced physical meaning to the nonrandomness factors.

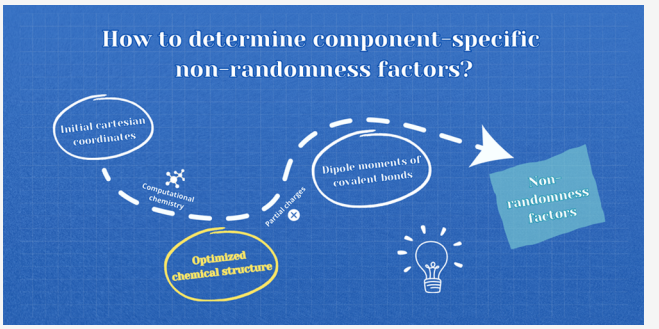

1. INTRODUCTION

Different excess Gibbs free energy thermodynamic models have been developed over the years comprising specific parameters in their entropic terms to describe the spatial randomness of the chemical species and their mixtures. The most well-known example is the Nonrandom Two-Liquid (NRTL) model, which was proposed by H. Renon and J.M. Prausnitz[1] in 1968 and takes into account the nonrandomness of the interactions between particles of similar and different types.[2,3] It is widely used to describe liquid−liquid equilibria (LLE)[4−6] and vapor−liquid equilibria (VLE)[7−10] and requires three parameters for a binary system: two binary interaction parameters (BIPs) and the nonrandomness factor (α).[11]

NRTL considers excess internal energy (U^E) equal to excess Gibbs free energy (G^E), bypassing proper thermodynamic integration, so G^E is given by eq 1.[3,11,12]

$$\frac{G^E}{RT} = \sum_i^M x_i \frac{\sum_j^M \tau_{ji} G_{ji} x_j}{\sum_j^N G_{ji} x_j} \quad (1)$$

where M is the number of components in the mixture, x_i and x_j are the mole fractions of species i and j, and G_{ij} is calculated using

$$G_{ij} = \exp\left[-\alpha_{ij} \cdot \frac{(g_{ij} - g_{jj})}{RT}\right] = \exp\left[-\alpha_{ij} \cdot \frac{\Delta g_{ij}}{RT}\right] = \exp(-\alpha_{ij} \cdot \tau_{ij}) \quad (2)$$

where g_{ij} and g_{jj} are the interaction energy parameters, which refer to the i−j and j−j interactions, respectively, and α_{ij} is the

Special Issue: In Honor of Maria Eugenia Macedo

Received: September 4, 2023
Revised: November 8, 2023
Accepted: November 21, 2023
Published: December 12, 2023

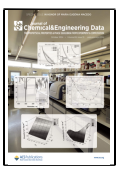

Table 1. Collected Liquid−Liquid Equilibria Data, at T = 298.15 K and P = 0.1 MPa, for Ternary Systems Containing Neutral Molecules Only

system no.	species 1	species 2	species 3	no. points	range of x_1 in phase I	range of x_2 in phase II	ref
1	butan-1-ol	ethanol	water	36	0.1202−0.4853	0.0000−0.0609	33
2	benzene	ethanol	water	26	0.4502−0.9877	0.0471−0.4126	34
3	dibutyl ether	propan-1-ol	water	16	0.0467−0.9311	0.0102−0.0973	35
4	dibutyl ether	methanol	water	22	0.4862−0.9694	0.0329−0.6829	35
5	glycerol	benzene	propan-1-ol	24	0.0000−0.1350	0.0086−0.0518	36
6	glycerol	benzene	ethanol	24	0.0000−0.0671	0.0086−0.1310	36
7	glycerol	benzene	methanol	22	0.0000−0.0079	0.0086−0.1370	36
8	methyl tert-butyl ether	hexan-1-ol	water	22	0.0000−0.9098	0.0000−0.0026	37
9	methyl tert-butyl ether	ethanol	water	12	0.1982−0.9259	0.0000−0.1331	37
10	*n*-heptane	toluene	sulfolane	20	0.2390−0.9080	0.0340−0.4380	38
11	*n*-nonane	o-xylene	butane-1,4-diol	16	0.0000−0.0080	0.1110−0.9890	39
12	*n*-nonane	o-xylene	glycerol	14	0.0000−0.0020	0.0920−0.9920	39
13	water	ethanol	*n*-amyl acetate	16	0.7687−1.0000	0.0000−0.3454	40
14	water	methanol	*n*-amyl acetate	16	0.5869−1.0000	0.0000−0.3825	40
15	water	methanol	toluene	22	0.0047−0.0162	0.0140−0.6424	41

nonrandomness factor, *i.e.*, an adjustable parameter related to the randomness of the spatial orientation of the interacting particles.

The nonrandomness factor (α_{ij}) is commonly determined based on, for example, liquid−liquid equilibria (LLE) data[11] or simply arbitrated between 0 (completely random spatial orientation of the particles) and 1 (completely defined/dependent spatial orientation), with most common applications being from 0.20 to 0.47.[1,8,13] Nevertheless, no proper methodology has been developed to calculate the nonrandomness factor, and inadequate values of this parameter have been found to cause convergence issues[3] and to hamper accurate description of extrema (such as azeotropes).[8]

Other more indirect application of parameters related to the randomness of mixtures is the Universal Quasi-chemical (UNIQUAC) model, which was developed by D.S. Abrams and J.M. Prausnitz in 1975.[14] It is a local composition model based on the two-fluid theory and is capable of representing vapor−liquid equilibria (VLE)[15−18] and liquid−liquid equilibria (LLE)[4,5,19−21] of mixtures.[14,22] UNIQUAC was deduced from a statistical mechanics basis, extending Guggenheim's quasi-chemical theory,[14,23] and building on the work of Wilson.[24]

According to UNIQUAC, the excess Gibbs free energy (G^E) is the sum of combinatorial (G_C^E) and residual (G_R^E) contributions, as can be seen in eq 3. The combinatorial contribution (eq 4) accounts for both size and shape effects, while the residual contribution (eq 5) accounts for interactions among molecules.[14]

$$G^{E,\mathrm{UNIQUAC}} = G_C^E + G_R^E \tag{3}$$

$$\frac{G_C^E}{RT} = \sum_{i=1}^{n_{species}} \left[x_i \ln\left(\frac{\phi_i}{x_i}\right)\right] - \frac{Z}{2} \sum_{i=1}^{n_{species}} q_i x_i \ln\left(\frac{\theta_i}{\phi_i}\right) \tag{4}$$

$$\frac{G_R^E}{RT} = -\sum_{i=1}^{n_{species}} q_i x_i \ln\left(\sum_{j=1}^{n_{species}} \theta_j \tau_{ji}\right) \tag{5}$$

where x_i is the mole fraction of component i, $n_{species}$ is the number of species in solution, Z is the lattice coordination number, ϕ and θ are the average volume fraction and average local area fraction of component i, respectively, r_i and q_i are the UNIQUAC volume and area parameters, respectively, and τ_{ij} are the UNIQUAC binary interaction parameters relative to the pair ij.

The UNIQUAC parameters τ_{ij} can be calculated from the interaction energies between species i and j, noted as U_{ij}, following eq 6.[14]

$$\tau_{ij} = e^{-(Z/2)[(U_{ij}-U_{jj})/(RT)]} = e^{-(Z/2)[\Delta U_{ij}/(RT)]} \tag{6}$$

Concerning the lattice coordination number (Z), which appears in both combinatorial and residual terms, it is defined as 10 for liquids, which was considered an intermediate value between 8 and 12 (the boundaries for Z in the liquid state).[3,14] Theoretically, the lattice coordination number is related to the nonrandomness factor by eq 7,[3] so nonrandomness factors should reside in the range $0.17 \leq \alpha \leq 0.33$.[3] Nevertheless, the $Z/2$ term in eq 6 is considered a too extreme correction to nonrandomness, and accurate methodologies to calculate this parameter still have to be developed, so this term is often ignored.[3,13]

$$Z = \frac{2}{\alpha} \tag{7}$$

Generally, the parameters of thermodynamic models have a well-defined physical meaning, for which they can be related to macroscopic properties of the system or to microscopic properties of the chemical components using different approaches. Density Functional Theory (DFT) is a computational quantum mechanical modeling methodology used in various fields of physics, chemistry, and materials science, which descends from the methods of Thomas−Fermi and Hartree−Fock−Slater.[25] Furthermore, DFT is an *ab initio* simulation method, *i.e.*, it can predict material properties for new systems without any experimental input, so its primary application is to investigate the electronic (or nuclear) structure of many-body systems, such as atoms and molecules. DFT structure optimization is used to determine the most stable configuration of a molecule by minimizing its energy, which involves an iterative adjustment of the positions of the atoms considering the electron density probability function as a variable, in contrast with wave function methods, which are unfeasible for large systems.[25,26]

Since its development in the second half of the 20th century, DFT has been employed, for example, in the description of ionic liquids[27−29] and in the optimization of materials in catalysis,

https://doi.org/10.1021/acs.jced.3c00532
J. Chem. Eng. Data 2024, 69, 3573−3583

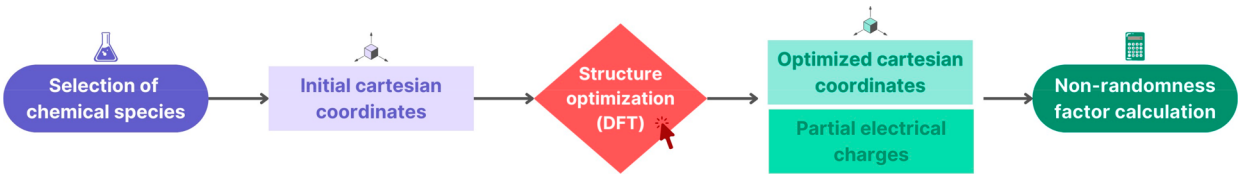

Figure 1. Novel methodology for the calculation of nonrandomness factors (α).

photochemistry, and surface chemistry.[30−32] However, even though DFT requires relatively low computational effort and has accurate predictive power,[25] its application has been limited by the approximations used in hybrid functionals and by the long-time needed for calculations in the liquid state.[26]

In this work, a novel geometric methodology based on computational chemistry, named Porto's approach, was proposed and applied in the calculation of the nonrandomness factors for 50 pure chemical species in the liquid state. Then, the traditional methods (α = 0.2 or 0.3 for NRTL and α = 0.2 for UNIQUAC) were compared against the usage of a component-specific nonrandomness factor in the correlation of liquid−liquid equilibria (LLE) data for 15 ternary systems comprising solely neutral molecules.

2. MATERIALS AND METHODS

2.1. Collected LLE Data. Table 1 shows the liquid−liquid equilibrium (LLE) data of the studied ternary systems, which were limited to neutral species to allow a clearer comparison of the different correlation approaches. The full data sets can be found in Table S1,[33−41] in the Supporting Information.

2.2. Porto's Approach for Calculating the Nonrandomness Factor. The nonrandomness factor (α) of each chemical species was estimated using a novel approach based on computational chemistry. First, the geometry of each molecule was optimized by using Density Functional Theory (DFT). Then, the Cartesian coordinates of each atom, as well as the respective electrical charges, were obtained from the optimized geometry, which allowed the determination of the dipole moment of each molecule and the respective nonrandomness factor. The overall methodology is summarized in Figure 1 and the studied chemical species can be observed in Table 2.

To perform the chemical structure optimizations, computations were performed at DFT level of theory using the Gaussian G09 R-D.01 software.[47] In this work, a combination of the DFT hybrid functional B3LYP[42,43] with the basis set 6-311++G[48] was used. The molecules were considered to be in a cavity within a liquid solvent composed of molecules of their own, and solvation was described according to the Polarizable Continuum Model (PCM).[44−46] This model is used to simulate the solute cavity via a set of overlapping spheres and requires the knowledge of dielectric constants, refractive indices, densities, and molar masses for each chemical species, which can be seen in Table S2,[49−100] in the Supporting Information. In addition, after the geometry optimization, a population analysis of the electrons was performed using the Natural Bond Orbital (NBO) function[101] to determine orbital electronic densities and the consequent electrical charge distribution. Afterward, the overall dipole moment (or electronic asymmetry) of each molecule was calculated using eq 8.

$$\vec{A} = \sum_{i}^{n_{\text{bonds}}} [(\delta q_i - \delta q_j)\cdot \vec{d}_{ij}] \tag{8}$$

Table 2. Chemical Species and Models Used in DFT Calculations with the B3LYP[42,43] + PCM[44−46] Model

species	chemical formula	CAS No.
acetonitrile	C_2H_3N	75-05-08
aniline	C_6H_7N	62-53-3
benzaldehyde	C_7H_6O	100-52-7
benzene	C_6H_6	71-43-2
butan-1-ol	$C_4H_{10}O$	71-36-3
butan-2-one	C_4H_8O	78-93-3
butane-1,4-diol	$C_{10}H_{20}O_6$	25103-87-1
butylamine	$C_4H_{11}N$	109-73-9
cumene	C_9H_{12}	98-82-8
cyclohexane	C_6H_{12}	110-82-7
cyclohexanone	$C_6H_{10}O$	108-94-1
decan-1-ol	$C_{10}H_{22}O$	112-30-1
dibutyl ether	$C_8H_{18}O$	142-96-1
dimethoxyethane	$C_4H_{10}O_2$	110-71-4
dodecan-1-ol	$C_{12}H_{26}O$	112-53-8
ethanol	C_2H_5OH	64-17-5
ethyl lactate	$C_5H_{10}O_3$	687-47-8
glycerol	$C_3H_8O_3$	56-81-5
heptan-1-ol	$C_7H_{16}O$	111-70-6
heptan-2-one	$C_7H_{14}O$	110-43-0
hexan-1-ol	$C_6H_{14}O$	111-27-3
hexan-2-one	$C_6H_{12}O$	591-78-6
m-cresol	C_7H_8O	108-39-4
m-xylene	C_8H_{10}	108-38-3
methanol	CH_4O	67-56-1
methyl *tert*-butyl ether	$C_5H_{12}O$	1634-04-4
n-amyl acetate	$C_7H_{14}O_2$	628-63-7
n-decane	$C_{10}H_{22}$	124-18-5
n-formylmorpholine	$C_5H_9NO_2$	4394-85-8
n-heptane	C_7H_{16}	142-82-5
n-hexane	C_6H_{14}	110-54-3
n-nonane	C_9H_{20}	111-84-2
n-octane	C_8H_{18}	111-65-9
n-pentane	C_5H_{12}	109-66-0
nonan-1-ol	$C_9H_{20}O$	143-08-8
o-xylene	C_8H_{10}	95-47-6
octan-1-ol	$C_8H_{18}O$	111-87-5
p-xylene	C_8H_{10}	106-42-3
pentan-1-ol	$C_5H_{12}O$	71-41-0
pentan-2-one	$C_5H_{10}O$	107-87-9
propan-1-ol	C_3H_8O	71-23-8
propan-2-ol	C_3H_8O	67-63-0
propan-2-one	C_3H_6O	67-64-1
propylamine	C_3H_9N	107-10-8
pyridine	C_5H_5N	110-86-1
quinoline	C_9H_7N	91-22-5
sulfolane	$C_4H_8O_2S$	126-33-0
toluene	C_7H_8	108-88-3
undecan-1-ol	$C_{11}H_{24}O$	112-42-5
water	H_2O	7732-18-5

https://doi.org/10.1021/acs.jced.3c00532
J. Chem. Eng. Data 2024, 69, 3573−3583

where $\vec{A}$ is the electronic asymmetry (in C·m), δq_i and δq_j are the partial charges of the bonded atoms ij (in C) obtained from DFT calculations, and $\vec{d}_{ij}$ is the distance vector between the two atoms (in m) along the 3 axes (x,y,z).

Therefore, the asymmetry ($\vec{A}$) can be written as a function of the three unitary vectors of each Cartesian axis, as shown in eq 9.

$$\vec{A} = a_x\vec{i} + a_y\vec{j} + a_z\vec{k} \tag{9}$$

The nonrandomness factor of each molecule was estimated using eq 10, which yields a normalized ratio of the determined electronic asymmetry components in the three axes (a_x, a_y, and a_z) by the maximum obtainable asymmetry in each direction.

$$\alpha = \frac{1}{3}\left(\frac{|a_x|}{a_{x,\max}} + \frac{|a_y|}{a_{y,\max}} + \frac{|a_z|}{a_{z,\max}}\right) \tag{10}$$

where $a_{x,\max}$, $a_{y,\max}$, and $a_{z,\max}$ denote the components of $\vec{A}_{\max}$ along the x, y, and z axes, respectively, which was determined using eq 11.

$$\vec{A}_{\max} = \sum_{i}^{n_{\text{bonds}}} |\delta q_i - \delta q_j|\cdot|\vec{d}_{ij}| \tag{11}$$

where $\vec{A}_{\max}$ is the maximum obtainable electronic asymmetry, which would happen in the hypothetical case of all chemical bonds contributing to increase the dipole moment (named as reference state), as Figure 2 shows.

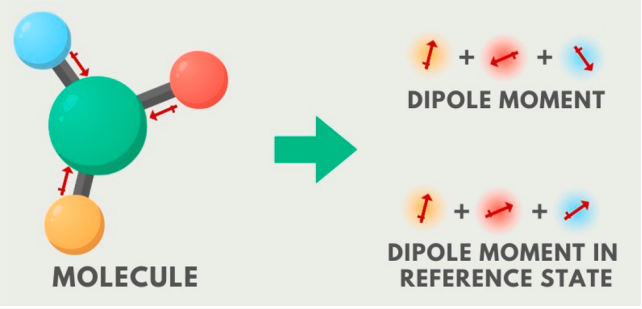

Figure 2. Example of determination of the dipole moment for the reference state (*i.e.*, maximum electronic asymmetry).

The nonrandomness factor of mixtures (α_{mix}) can then be calculated following the mixing rule given by the weighted mean of eq 12.

$$\alpha_{\text{mix}} = \sum_{i=1}^{n_{\text{species}}} \alpha_i x_i \tag{12}$$

where α_i and x_i are the nonrandomness factor and the mole fraction of species i, respectively.

2.3. LLE Data Correlation Using NRTL and UNIQUAC.

The NRTL model was applied using fixed values of the nonrandomness factors (α = 0.2 and 0.3), as it is commonly performed in literature, and using component-specific values, which were determined following the approach explained in section 2.2. This latter methodology was designated as pNRTL (Porto's approach on NRTL) to ease discussion.

Concerning the UNIQUAC model, the volume (r) and area (q) parameters were calculated using eqs 13 and 14,[3] respectively.

$$r = \frac{V_w}{15.17 \times 10^{-6}} \tag{13}$$

$$q = \frac{A_w}{2.5 \times 10^{5}} \tag{14}$$

where V_w is the van der Waals surface volume (in m^3/mol) and A_w is the van der Waals surface area (in m^2/mol). These two parameters were calculated following the Bondi's method,[102] and values can be found in Table S3,[103] in the Supporting Information, together with the respective UNIQUAC r and q parameters, for all studied chemical species.

Moreover, all the lattice coordination numbers (Z) in the UNIQUAC equations were converted to nonrandomness factors following the relation of eq 7, so the model was applied considering α = 0.2 (Z = 10), which is the standard procedure, and considering the determined component-specific nonrandomness factors. Hence, eqs 4 to 6 had to be rewritten into eqs 15 to 17, respectively. In eq 15, seeing that the lattice coordination number (now converted to α) is no longer equal for all interacting species, the nonrandomness factor was moved to inside the summation. Similarly to NRTL and pNRTL, this new form of UNIQUAC was named pUNIQUAC (Porto's approach to UNIQUAC) to ease discussion.

$$\frac{G_C^E}{RT} = \sum_{i=1}^{n_{\text{species}}}\left[x_i \ln\left(\frac{\phi_i}{x_i}\right)\right] - \sum_{i=1}^{n_{\text{species}}}\frac{1}{\alpha_i}q_i x_i \ln\left(\frac{\theta_i}{\phi_i}\right) \tag{15}$$

$$\frac{G_R^E}{RT} = -\sum_{i=1}^{n_{\text{species}}} q_i x_i \ln\left(\sum_{j=1}^{n_{\text{species}}}\theta_j\tau_{ji}\right) \tag{16}$$

$$\tau_{ij} = e^{-1/\alpha_{ij}(U_{ij}-U_{jj})/RT} \tag{17}$$

where α_i stands for the nonrandomness factor of species i and α_{ij} for the mean nonrandomness factor between species i and j, which was calculated according to eq 18, *i.e.*, a particular case of eq 10 for binary interactions.

$$\alpha_{ij} = (\alpha_i + \alpha_j)/2 \tag{18}$$

All models were applied in the correlation of LLE data keeping in mind the general phase equilibrium condition, *i.e.*, the isoactivity criterion (IC) between the liquid phases, which is translated by eq 19. For that purpose, an algorithm was developed to optimize the binary interaction parameters (τ_{ij}) by minimizing the standard deviations from the collected LLE data, using eq 20, and with the constraint of fulfilling the IC. In this process, an interior-point convergence method was used with 1×10^8 maximum iterations and 1×10^8 maximum function evaluations. Then, the algorithm determined equilibrium phase composition using the optimized binary interaction parameters, preserving the fulfilment of the isoactivity criterion, and calculated the final standard deviations from the collected LLE data using eq 20. The overall procedure for the correlation of LLE data is summarized in Figure 3.

$$\text{IC} = \frac{\sum_{j=1}^{n_{\text{points}}}\sum_{i=1}^{n_{\text{species}}}\left(x_{ij}^{\text{corr,I}}\gamma_{ij}^{\text{I}} - x_{ij}^{\text{corr,II}}\gamma_{ij}^{\text{II}}\right)}{n_{\text{points}}\cdot n_{\text{species}}} = 0 \tag{19}$$

$$\sigma_x = \sqrt{\frac{\sum_{i=1}^{n_{\text{points}}}\sum_{j=1}^{n_{\text{species}}}\left(x_{ij}^{\text{corr}} - x_{ij}^{\text{lit}}\right)^2}{n_{\text{points}}\cdot n_{\text{species}}}} \tag{20}$$

https://doi.org/10.1021/acs.jced.3c00532
J. Chem. Eng. Data 2024, 69, 3573−3583

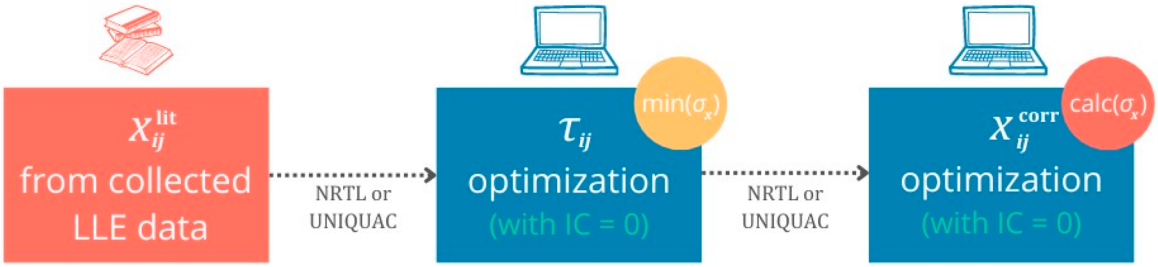

Figure 3. Overall procedure for the correlation of liquid−liquid equilibrium (LLE) data.

where n_{points} is the number of equilibria points in the system under study, $n_{species}$ is the number of chemical species present, x_{ij}^{corr} and x_{ij}^{lit} are, respectively, the correlated and literature-based mole fraction of species i in the data point j, and γ_{ij} is the activity coefficient of species i in the data point j. I and II refer to the two liquid phases in equilibrium.

3. RESULTS AND DISCUSSION

3.1. Calculating the Nonrandomness Factors. Following Porto's approach, the nonrandomness factors (α) were determined for the species comprised in the ternary systems shown in Table 1 and for some others, totalizing 50 chemical components, as Table 3 shows. In the calculations, density and dielectric constant were considered at 298.15 K and 0.1 MPa, so the obtained parameters refer to the pure liquid state at these conditions.

Table 3. Determined Nonrandomness Factors (α) for Pure Components at 298.15 K and 0.1 MPa

species	α	species	α
acetonitrile	0.0448	methyl *tert*-butyl ether	0.0415
aniline	0.3254	*n*-amyl acetate	0.0193
benzaldehyde	0.3479	*n*-decane	6.10×10^{-6}
benzene	0.1546	*n*-formylmorpholine	0.1140
butan-1-ol	0.1874	*n*-heptane	3.18×10^{-3}
butan-2-one	0.0389	*n*-hexane	6.42×10^{-6}
butane-1,4-diol	0.2426	*n*-nonane	2.62×10^{-3}
butylamine	0.1045	*n*-octane	1.20×10^{-4}
cumene	0.0132	*n*-pentane	4.05×10^{-3}
cyclohexane	9.84×10^{-7}	nonan-1-ol	0.1411
cyclohexanone	0.0535	o-xylene	9.11×10^{-3}
decan-1-ol	0.0620	octan-1-ol	0.1544
dibutyl ether	0.0530	*p*-xylene	2.97×10^{-6}
dimethoxyethane	0.1320	pentan-1-ol	0.1631
dodecan-1-ol	0.0585	pentan-2-one	0.0327
ethanol	0.2345	propan-1-ol	0.1970
ethyl lactate	0.1194	propan-2-ol	0.1119
glycerol	0.4630	propan-2-one	0.0326
heptan-1-ol	0.1482	propylamine	0.1246
heptan-2-one	0.0270	pyridine	0.1544
hexan-1-ol	0.1663	quinoline	0.1576
hexan-2-one	0.0292	sulfolane	5.14×10^{-3}
m-cresol	0.0811	toluene	0.0112
m-xylene	8.11×10^{-3}	undecan-1-ol	0.1362
methanol	0.3242	water	0.3333

As Table 3 shows, the largest nonrandomness factors were obtained for particularly polar molecules (such as glycerol and benzaldehyde), while the smallest were verified for very nonpolar molecules (such as *p*-xylene and *n*-decane), which exhibit a higher randomness of spatial orientation due to the lack of well-defined electrical dipoles. Regarding water, a nonrandomness factor of 0.3333 was obtained, *i.e.*, the optimal spatial conformation of water in the studied conditions (298.15 K and 0.1 MPa) could not cancel out 33.33% of what would have been the molecular dipole moment in its reference state. This result goes in line with the known polarity of water and is in surprising agreement with the very common application of α = 0.3 for aqueous mixtures (in which water is the most abundant component).

For linear 1-alcohols, *i.e.*, $CH_3(CH_2)_{n+1}OH$ with $n = -1-10$, a general decrease of the nonrandomness factor (α) was observed with decreasing dielectric constant and with growing length of the alkane chain, as Figure 4 illustrates. This is probably due to the rising nonpolar nature of the alkane chains, which gradually cancel out the dipole moment caused by the presence of the characteristic hydroxyl group (—OH) of alcohols. Moreover, no significant differences were observed between molecules with odd and even numbers of carbons, thus hinting similar and rather predictable behavior, except for decan-1-ol and docecan-1-ol, which presented very low nonrandomness factors. The appearance of low nonrandomness factors for these two species was already expected due to their low dipole moments (illustrated by the low dielectric constants in Figure 4 and Table S2) which are caused by the complete neutralization of the dipole moment of the —OH bond. Therefore, linear alcohols with long alkyl chains become practically nonpolar, increasing spatial randomness and decreasing the nonrandomness factors.

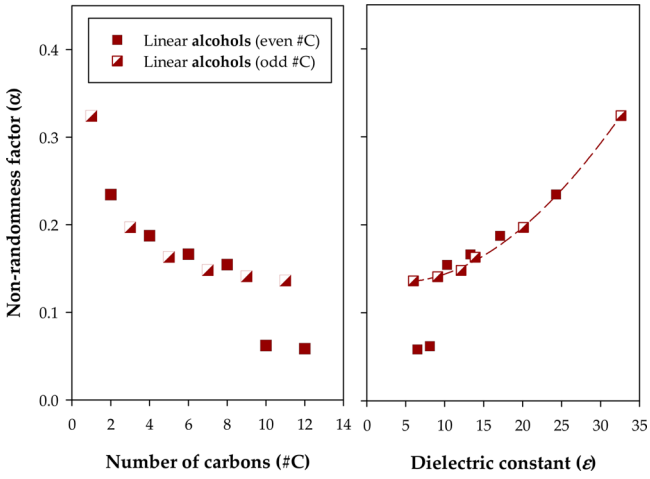

Figure 4. Influence of the number of carbon atoms (#C) and dielectric constant (ε) on the nonrandomness factor (α) at 298.15 K and 0.1 MPa for linear 1-alcohols, *i.e.*, $CH_3(CH_2)_{n+1}OH$ with $n = -1-10$.

https://doi.org/10.1021/acs.jced.3c00532
J. Chem. Eng. Data 2024, 69, 3573−3583

Similarly to what was observed for 1-alcohols, for linear alkanes ($CH_3(CH_2)_nCH_3$ with n = 3−8) and 2-ketones ($CH_3CO(CH_2)_nCH_3$ with n = 0−4), a general decrease of the nonrandomness factors was noticed with increasing length of the alkane chain and decreasing dielectric constant, as Figure 5

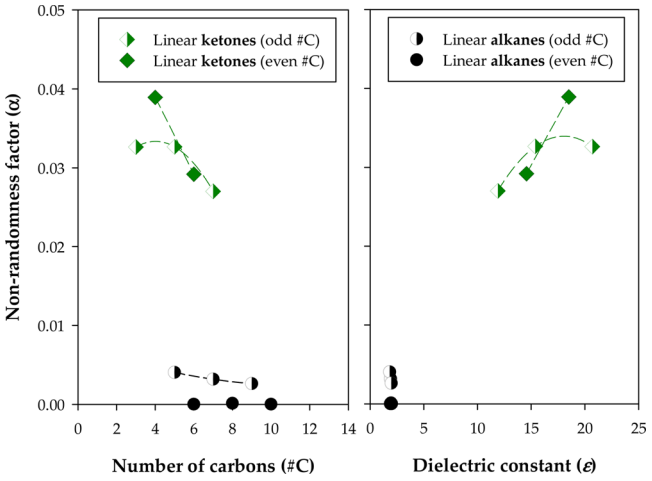

Figure 5. Influence of the number of carbon atoms (#C) and dielectric constant (ε) on the nonrandomness factor (α) at 298.15 K and 0.1 MPa for linear alkanes ($CH_3(CH_2)_nCH_3$ with n = 3−8) and 2-ketones ($CH_3CO(CH_2)_nCH_3$ with n = 0−4).

shows. The dielectric constant of a substance is related to its ability to accumulate electrical energy, which is favored by the presence of clear electric dipoles. Therefore, it is possible to conclude that more significant molecular dipoles cause a more defined spatial orientation of the molecules (*i.e.*, larger nonrandomness factors), which eases the storage of electrical energy (*i.e.*, larger dielectric constants).

When comparing some similar aromatics, the same trend was observed regarding the effect of the dielectric constants, so larger nonrandomness factors were linked to higher dielectric constants, as can be seen in Figure 6. Notoriously, benzene did not attain the lowest nonrandomness factor (*i.e.*, the most random spatial distribution) despite its well-known equal charge distribution among the carbon atoms. Substituting aromatic

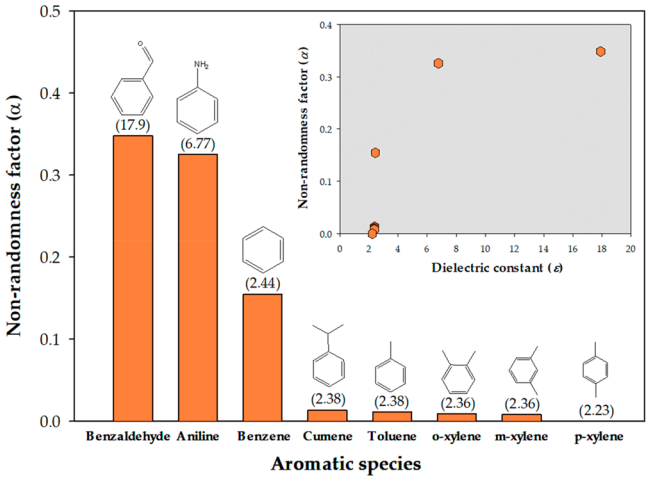

Figure 6. Determined nonrandomness factors (α) at 298.15 K and 0.1 MPa for some similar aromatic species, with respective chemical structures and dielectric constants at 298.15 K (in parentheses).

hydrogens by alkyl groups allowed for a larger area for the electronic cloud, probably decreasing the existent dipole moments, as can be observed for *p*-xylene, which had both the lowest dielectric constant and the lowest nonrandomness factor.

Although the proposed methodology showed very logical trends for the nonrandomness factor (α) with the dielectric constants and alkyl chain lengths, very low values of this parameter were obtained for nonpolar molecules such as *p*-xylene and *n*-alkanes, implying immensely large values of the lattice coordination number (Z). As is well-known, the lattice coordination number corresponds to the number of nearest neighbor molecules surrounding a certain particle, for which high magnitude values do not have any physical meaning. Nevertheless, it must be noted that the physical relationship between Z and α is only valid for small, close to spherical and up to moderately random molecules. The spatial arrangement of molecules with large atom chains cannot be determined simply by assessing polarity due to steric effects, and very random molecules do not get distributed following any intelligible pattern, so Z does not convey any relevant information in these cases.

From the observed so far, it is clear that determining a nonrandomness factor specific to each chemical species is feasible and that the dielectric constant seems to be a crucial factor. However, it is still necessary to evaluate the sensitivity of NRTL and UNIQUAC to this parameter in the correlation of the ternary liquid−liquid equilibria data.

3.2. LLE Correlation Using the Determined Nonrandomness Factors. To compare the methodology proposed in this work with the more classical approaches to the NRTL and UNIQUAC models, the liquid−liquid equilibria (LLE) data of the 15 ternary systems shown in Table 1 were correlated, and the obtained deviations, calculated by eq 20, were compared.

The standard deviations obtained for NRTL with α = 0.2 and α = 0.3, and with calculated nonrandomness factors (pNRTL), are shown in Figure 7. The obtained interaction energy parameters (Δg_{ij}) and standard deviations (σ_x) can be seen in Table S4, in the Supporting Information. As expected, the obtained standard deviations were very similar for all the

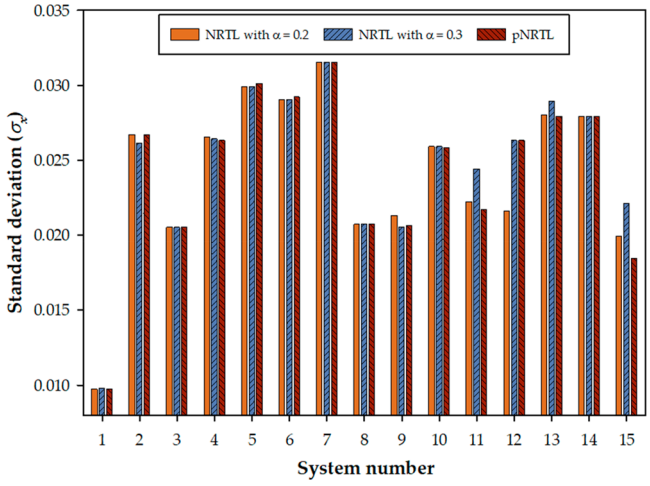

Figure 7. Standard deviations for NRTL with α = 0.2 and α = 0.3 and with calculated nonrandomness factors (pNRTL) obtained in the correlation of ternary liquid−liquid equilibria (LLE) data from literature.

https://doi.org/10.1021/acs.jced.3c00532
J. Chem. Eng. Data 2024, 69, 3573−3583

alternatives, revealing the known lack of sensitivity of NRTL toward the value of the nonrandomness factor.

Figure 8 illustrates the obtained standard deviations for UNIQUAC with α = 0.2 (Z = 10) and with calculated

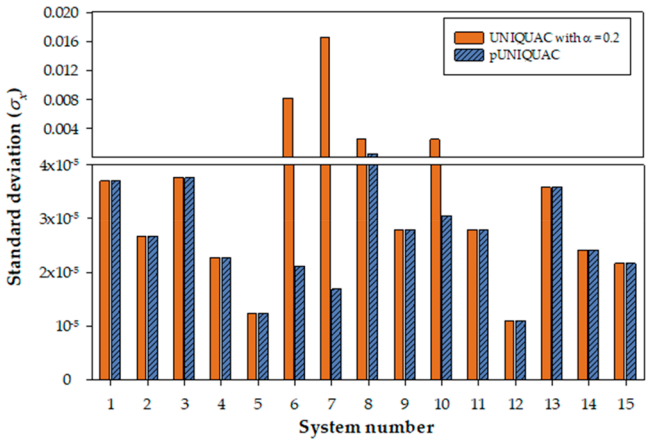

Figure 8. Standard deviations for UNIQUAC with $\alpha = 0.2$ ($Z = 10$) and with calculated nonrandomness factors ($Z = 2/\alpha$) in the correlation of ternary liquid−liquid equilibria (LLE) data from literature.

nonrandomness factors ($Z = 2/\alpha$) in the correlation of LLE data from literature. The interaction energy parameters (ΔU_{ij}) and standard deviations (σ_x) can be seen in Table S5 in the Supporting Information.

For most systems, UNIQUAC and pUNIQUAC achieved similar values of standard deviations, for which the inclusion of a component-specific nonrandomness factor did not significantly improve phase equilibria correlation. Nevertheless, pUNIQUAC always obtained equal or lower standard deviations than classical UNIQUAC, particularly to what concerned very polar (systems 6 and 7) and nonpolar (system 10) ternaries.

Furthermore, it was noticed that the correlation approaches based on UNIQUAC outperformed the ones of NRTL, suggesting that the former is more appropriate to the precise description of this type of systems. However, even though no problems related to very nonpolar molecules were noticed in the correlation of the LLE data, it must be referred that the pUNIQUAC model could present some difficulties when modeling species with almost null nonrandomness factors (α), which could cause extreme values in its combinatorial term given the form of eq 15. On the contrary, pNRTL only considers nonrandomness factors of binary interactions (α_{ij}), which make this model less prone to low values of this parameter. In fact, while α can present very low (close to 0) or high values (close to 1), α_{ij} is unlikely to do so given the necessity of immiscibility for the existence of liquid−liquid equilibria (*i.e.*, if all species present analogous spatial randomness, then they are probably completely miscible). Nevertheless, an alternative version of eq 15 could be used for the description of very nonpolar mixtures, considering the mean nonrandomness factor of mixture (eq 12), which is given by eq 21. Yet, this equation is considered to have a weaker theoretical foundation since the combinatorial term should account for each species separately.

$$\frac{G_C^E}{RT} = \sum_{i=1}^{n_{species}} \left[x_i \ln\left(\frac{\phi_i}{x_i}\right)\right] - \frac{1}{\alpha_{mix}} \sum_{i=1}^{n_{species}} q_i x_i \ln\left(\frac{\theta_i}{\phi_i}\right) \quad (21)$$

From the original theories, it is clear that the binary interaction parameters (BIPs) of the UNIQUAC and NRTL models would translate the energy of the binary interactions between each pair of species. However, even when limiting the number of parameters and their reasonable dominium, BIPs cannot be regarded as trustworthy description of the energetic interactions due to the nonunique feasible combinations of parameters with similar value of excess Gibbs free energy. In other words, the mathematical expressions of the excess Gibbs free energy are not injective functions, and, for that reason, BIPs should be seen as mathematical parameters with significant dependence on the optimization algorithm and should not be given any specific physical meaning.

The inclusion of the nonrandomness factor (α) in NRTL and of the lattice coordination number (Z) in UNIQUAC is essential to reduce the number of feasible combinations of BIPs with equal value of excess Gibbs free energy, but the effect of this term has been limited by the consideration of an equal value for all chemical species. Hence, even though similar standard deviations were obtained for the classical and modified versions of UNIQUAC and NRTL, pUNIQUAC and pNRTL could strengthen the physical fundament of the nonrandomness factors and promote more injective excess Gibbs free energy functions, making them important assets in moving these models further away from simple mathematical correlations and closer to predictive models. Moreover, the parameters calculated following the proposed methodology are expected to convey a better characterization of mixtures by allowing prediction of nonideality and better description of azeotropes, and infer solubilities.

4. CONCLUSIONS

The application of thermodynamic models such as nonrandom two-liquid (NRTL) and Universal Quasi Chemical (UNIQUAC) in the description of phase equilibria is often hindered by the inclusion of fixed values for parameters which could have been calculated based on their well-defined physical meaning, making the prediction of equilibrium composition in the absence of copious experimental data very problematic.

The nonrandomness factor (α) is a parameter which appears in both the NRTL and UNIQUAC models. It is related to the randomness of the spatial orientation of the chemical species and, consequently, to the randomness of the surrounding local composition. Theoretically, it goes from 0 (completely random spatial orientation of the particles) to 1 (completely defined/dependent spatial orientation), but most applications fix this parameter between 0.20 and 0.47 due to the lack of reliable methodologies for its estimation.

In this work, an innovative methodology used computational chemistry to determine the nonrandomness factors of 50 chemical species at 298.15 K, 0.1 MPa and liquid state. As expected, larger values of these parameters were obtained for more polar molecules such as glycerol (α = 0.4630) and water (α = 0.3333), while more nonpolar molecules such as such as *p*-xylene and *n*-decane presented practically null values. Polar molecules are known for their well-defined electrical dipoles, which cause a preferential spatial orientation when in solution, increasing the values of the nonrandomness factors.

Finally, the validity of the determined parameters was tested by correlating liquid−liquid equilibria (LLE) of 15 ternary systems, and it was concluded that the proposed methodology would provide more specific nonrandomness factors, which are expected to ease the interpretation of phase equilibria by better

https://doi.org/10.1021/acs.jced.3c00532
J. Chem. Eng. Data 2024, 69, 3573−3583

describing azeotropes, hinting nonideality, and allowing to infer solubility.

■ ASSOCIATED CONTENT

Supporting Information

The Supporting Information is available free of charge at https://pubs.acs.org/doi/10.1021/acs.jced.3c00532.

Ternary liquid−liquid equilibria (LLE) data collected from literature; dielectric constants and densities (at 298.15 K and 0.1 MPa); the molar masses, the van der Waals surface volumes (V_w) and areas (A_w), together with the respective UNIQUAC volume (r) and area (q) parameters for 50 chemical species; interaction energy parameters (Δg_{ij} and ΔU_{ij}) and standard deviations from experimental data obtained in the correlation of LLE data (σ_x) (PDF)

■ AUTHOR INFORMATION

Corresponding Author

Pedro Velho − *LSRE-LCM−Laboratory of Separation and Reaction Engineering−Laboratory of Catalysis and Materials, Faculty of Engineering, University of Porto, 4200-465 Porto, Portugal; ALiCE−Associate Laboratory in Chemical Engineering, Faculty of Engineering, University of Porto, 4200-465 Porto, Portugal;* orcid.org/0000-0003-4802-7301; Email: velho@fe.up.pt

Authors

Leonor R. Barroca − *LSRE-LCM−Laboratory of Separation and Reaction Engineering−Laboratory of Catalysis and Materials, Faculty of Engineering, University of Porto, 4200-465 Porto, Portugal; ALiCE−Associate Laboratory in Chemical Engineering, Faculty of Engineering, University of Porto, 4200-465 Porto, Portugal;* orcid.org/0000-0002-0613-4208

Eugénia A. Macedo − *LSRE-LCM−Laboratory of Separation and Reaction Engineering−Laboratory of Catalysis and Materials, Faculty of Engineering, University of Porto, 4200-465 Porto, Portugal; ALiCE−Associate Laboratory in Chemical Engineering, Faculty of Engineering, University of Porto, 4200-465 Porto, Portugal;* orcid.org/0000-0002-0724-5380

Complete contact information is available at: https://pubs.acs.org/10.1021/acs.jced.3c00532

Notes

The authors declare no competing financial interest.

■ ACKNOWLEDGMENTS

This work was financially supported by UIDB/50020/2020 and UIDP/50020/2020 (LSRE-LCM), and LA/P/0045/2020 (ALiCE), funded by national funds through FCT/MCTES (PIDDAC). Pedro Velho thanks FCT [2021.06626.BD] for financial support. Leonor R. Barroca is grateful to the project 2Smart [NORTE-01-0145-FEDER-000054], supported by Norte Portugal Regional Operational Programme (NORTE 2020), under the PORTUGAL 2020 Partnership Agreement, through the European Regional Development Fund (ERDF).

■ REFERENCES

(1) Renon, H.; Prausnitz, J. M. Local compositions in thermodynamic excess functions for liquid mixtures. *AIChE J.* **1968**, *14*, 135−144.

(2) Assael, M. J.; Trusler, J. P. M.; Tsolakis, T. F. Activity Coefficient Models. *Thermophysical Properties of Fluids* **1996**, *1*, 161−206.

(3) Kontogeorgis, G. M.; Folas, G. K. *Thermodynamic Models for Industrial Applications: From Classical and Advanced Mixing Rules to Association Theories*; Wiley, 2010. DOI: 10.1002/9780470747537.

(4) Cháfer, A.; Torre, J.d.l.; Montón, J. B.; Lladosa, E. Experimental Determination and Correlation of Liquid−Liquid Equilibria Data for a System of Water + Ethanol + 1-Butyl-3-methylimidazolium Hexafluorophosphate at Different Temperatures. *J. Chem. Eng. Data* **2017**, *62*, 773−779.

(5) Simoni, L. D.; Lin, Y.; Brennecke, J. F.; Stadtherr, M. A. Modeling Liquid-Liquid Equilibrium of Ionic Liquid Systems with NRTL, Electrolyte-NRTL, and UNIQUAC. *Ind. Eng. Chem. Res.* **2008**, *47*, 256−272.

(6) del Mar Olaya, M.; Carbonell-Hermida, P.; Trives, M.; Labarta, J. A.; Marcilla, A. Liquid−Liquid Equilibrium Data Correlation Using NRTL Model for Different Types of Binary Systems: Upper Critical Solution Temperature, Lower Critical Solution Temperature, and Closed Miscibility Loops. *Ind. Eng. Chem. Res.* **2020**, *59*, 8469−8479.

(7) Ferreira, M.; Schwarz, C. E. Low-Pressure VLE Measurements and Thermodynamic Modeling, with PSRK and NRTL, of Binary 1-Alcohol + n-Alkane Systems. *J. Chem. Eng. Data* **2018**, *63*, 4614−4625.

(8) de Klerk, D. L.; Schwarz, C. E. Simplified Approach to Understanding, Evaluating, and Parameterizing the NRTL Model for the Description of Binary VLE: T$\tau\tau$-VLE Approach. *Ind. Eng. Chem. Res.* **2023**, *62*, 10629−10643.

(9) Zhao, Y.; Dong, X.; Gong, M.; Li, H.; Zhong, Q.; Shen, J. Evaluation of PR, NRTL, UNIFAC, and PCSAFT on the VLE of Binary Systems Containing Ammonia. *Ind. Eng. Chem. Res.* **2017**, *56*, 2287−2297.

(10) Du Plessis, S. H.; Latsky-Galloway, C.; Schwarz, C. E. Experimental Measurement and PSRK and NRTL Modeling of Binary 1-Alcohol (Cm) + n-Alkane (Cm+3) Vapor−Liquid Equilibrium Data. *J. Chem. Eng. Data* **2022**, *67*, 1915−1931.

(11) Chaves, I. D. G.; López, J. R. G.; Zapata, J. L. G.; Robayo, A. L.; Niño, G. R. Thermodynamic and Property Models. In *Process Analysis and Simulation in Chemical Engineering*; Springer International Publishing, 2016; pp 53−102.

(12) Dadmohammadi, Y.; Gebreyohannes, S.; Neely, B. J.; Gasem, K. A. M. Multicomponent phase behavior predictions using QSPR-generalized NRTL and UNIQUAC models. *Fluid Phase Equilib.* **2016**, *409*, 318−326.

(13) Prausnitz, J. M.; Lichtenthaler, R. N.; Azevedo, E.G.d. *Molecular Thermodynamics of Fluid-Phase Equilibria*; Prentice Hall International, 1999.

(14) Abrams, D. S.; Prausnitz, J. M. Statistical thermodynamics of liquid mixtures: A new expression for the excess Gibbs energy of partly or completely miscible systems. *AlChE J.* **1975**, *21*, 116−128.

(15) Saquete, M. D.; Font, A.; García-Cano, J.; Blasco, I. Study of the LLE, VLE, and VLLE of the Ternary System Water + 1-Butanol + Isoamyl Alcohol at 101.3 kPa. *J. Chem. Eng. Data* **2018**, *63*, 3733−3743.

(16) Kato, R.; Gmehling, J. Measurement and correlation of vapor−liquid equilibria of binary systems containing the ionic liquids [EMIM][(CF3SO2)2N], [BMIM][(CF3SO2)2N], [MMIM]-[(CH3)2PO4] and oxygenated organic compounds respectively water. *Fluid Phase Equilib.* **2005**, *231*, 38−43.

(17) Gomis, V.; Font, A.; Saquete, M. D.; García-Cano, J. LLE, VLE and VLLE data for the water−n-butanol−n-hexane system at atmospheric pressure. *Fluid Phase Equilib.* **2012**, *316*, 135−140.

(18) Garcia-Cano, J.; Saquete, M. D. Liquid-liquid, vapor-liquid and vapor-liquid-liquid experimental equilibrium of the system water + 1-butanol + 2-butanol at 101.3 kPa and data correlation. *Fluid Phase Equilib.* **2020**, *517*, 112617.

(19) Velho, P.; Requejo, P. F.; Gómez, E.; Macedo, E. A. Thermodynamic study of ATPS involving ethyl lactate and different inorganic salts. *Sep. Purif. Technol.* **2021**, *275*, 119155.

(20) Requejo, P. F.; Velho, P.; Gómez, E.; Macedo, E. A. Study of Liquid-Liquid Equilibrium of Aqueous Two-Phase Systems Based on

Ethyl Lactate and Partitioning of Rutin and Quercetin. *Ind. Eng. Chem. Res.* **2020**, *59*, 21196−21204.
(21) Rios, R. B.; Neto, A. A. E.; Medeiros, H. A. D.; Silva, F. F. M.; Oliveira, H. N. M.; Neto, E. L. B.; Chiavone-Filho, O. Liquid−Liquid Equilibria of Glycerol + Alcohol + Safflower Biodiesel Systems: Measurement and Modeling. *J. Chem. Eng. Data* **2023**, *68*, 1716−1727.
(22) Kontogeorgis, G. M.; Folas, G. K. Activity Coefficient Models Part 2: Local Composition Models, from Wilson and NRTL to UNIQUAC and UNIFAC. *Thermodynamic Models for Industrial Applications* **2010**, 109−157.
(23) Guggenheim, E. A. *Mixtures: The theory of the equilibrium properties of some simple classes of mixtures solutions and alloys*; Claredon Press Oxford, 1952.
(24) Wilson, G. M. Vapor-Liquid Equilibrium. XI. A New Expression for the Excess Free Energy of Mixing. *J. Am. Chem. Soc.* **1964**, *86*, 127−130.
(25) Kohn, W.; Becke, A. D.; Parr, R. G. Density Functional Theory of Electronic Structure. *J. Phys. Chem.* **1996**, *100*, 12974−12980.
(26) Burke, K. Perspective on density functional theory. *J. Chem. Phys.* **2012**, *136*, 150901.
(27) Philippi, F.; Quinten, A.; Rauber, D.; Springborg, M.; Hempelmann, R. Density Functional Theory Descriptors for Ionic Liquids and the Introduction of a Coulomb Correction. *J. Phys. Chem. A* **2019**, *123*, 4188−4200.
(28) Voroshylova, I. V.; Teixeira, F.; Costa, R.; Pereira, C. M.; Cordeiro, M. N. D. S. Interactions in the ionic liquid [EMIM][FAP]: a coupled experimental and computational analysis. *Phys. Chem. Chem. Phys.* **2016**, *18*, 2617−2628.
(29) Moosavi, M.; Banazadeh, N.; Torkzadeh, M. Structure and Dynamics in Amino Acid Choline-Based Ionic Liquids: A Combined QTAIM, NCI, DFT, and Molecular Dynamics Study. *J. Phys. Chem. B* **2019**, *123*, 4070−4084.
(30) Jensen, P. B.; Bialy, A.; Blanchard, D.; Lysgaard, S.; Reumert, A. K.; Quaade, U. J.; Vegge, T. Accelerated DFT-Based Design of Materials for Ammonia Storage. *Chem. Mater.* **2015**, *27*, 4552−4561.
(31) Ghogare, A. A.; Debaz, C. J.; Silva Oliveira, M.; Abramova, I.; Mohapatra, P. P.; Kwon, K.; Greer, E. M.; Prado, F. M.; Valerio, H. P.; Di Mascio, P.; Greer, A. Experimental and DFT Computational Insight into Nitrosamine Photochemistry-Oxygen Matters. *J. Phys. Chem. A* **2017**, *121*, 5954−5966.
(32) Roos, G.; Loverix, S.; De Proft, F.; Wyns, L.; Geerlings, P. A Computational and Conceptual DFT Study of the Reactivity of Anionic Compounds: Implications for Enzymatic Catalysis. *J. Phys. Chem. A* **2003**, *107*, 6828−6836.
(33) van Berlo, M.; Gude, M. T.; van der Wielen, L. A. M.; Luyben, K. C. A. M. Partition Coefficients and Solubilities of Glycine in the Ternary Solvent System 1-Butanol + Ethanol + Water. *Ind. Eng. Chem. Res.* **1997**, *36*, 2474−2482.
(34) Varteressian, K. A.; Fenske, M. R. Liquid-Liquid Extraction Performance of a Packed Extraction Column, Using Continuous Countercurrent. *Ind. Eng. Chem. Res.* **1936**, *28*, 928−933.
(35) Park, S.-J.; Hwang, I.-C.; Kwak, H.-Y. Binary Liquid-Liquid Equilibrium (LLE) for Dibutyl Ether (DBE) + Water from (288.15 to 318.15) K and Ternary LLE for Systems of DBE + C1 ∼ C4 Alcohols + Water at 298.15 K. *J. Chem. Eng. Data* **2008**, *53*, 2089−2094.
(36) Katayama, H.; Satoh, T. Liquid−Liquid Equilibria of Three Ternary Systems: {Glycerol + Benzene + Methanol}, {Glycerol + Benzene + Ethanol}, and {Glycerol + Benzene + 1-Propanol}. *J. Chem. Eng. Data* **2015**, *60*, 828−835.
(37) Ashour, I. Liquid-Liquid Equilibrium of MTBE + Ethanol + Water and MTBE + 1-Hexanol + Water over the Temperature Range of 288.15 to 308.15 K. *J. Chem. Eng. Data* **2005**, *50*, 113−118.
(38) Chen, J.; Li, Z.; Duan, L. Liquid-Liquid Equilibria of Ternary and Quaternary Systems Including Cyclohexane, 1-Heptene, Benzene, Toluene, and Sulfolane at 298.15 K. *J. Chem. Eng. Data* **2000**, *45*, 689−692.
(39) Brijmohan, N.; Moodley, K.; Narasigadu, C. Ternary Liquid−Liquid Equilibrium Data for the n-Nonane + o-Xylene + (Butane-1,4-diol or Glycerol) Systems at (298.2, 313.2, 333.2) K and 0.1 MPa. *J. Chem. Eng. Data* **2022**, *67*, 3468−3475.
(40) Arce, A.; Blanco, A.; Martínez-Ageitos, J.; Vidal, I. LLE data for the systems water + (methanol or ethanol) + n-amyl acetate. *Fluid Phase Equilib.* **1995**, *109*, 291−297.
(41) Tamura, K.; Chen, Y.; Yamada, T. Ternary and Quaternary Liquid-Liquid Equilibria for Fuel Additives of the Water + Methanol + Toluene and Water + Methanol + Toluene + Methyl tert-Butyl Ether or tert-Amyl Methyl Ether Systems at 298.15 K. *J. Chem. Eng. Data* **2001**, *46*, 1381−1386.
(42) Becke, A. D. Density-functional thermochemistry. III. The role of exact exchange. *J. Chem. Phys.* **1993**, *98*, 5648−5652.
(43) Lee, C.; Yang, W.; Parr, R. G. Development of the Colle-Salvetti correlation-energy formula into a functional of the electron density. *Phys. Rev. B: Condens. Matter Mater. Phys.* **1988**, *37*, 785−789.
(44) Miertuš, S.; Scrocco, E.; Tomasi, J. Electrostatic interaction of a solute with a continuum. A direct utilizaion of AB initio molecular potentials for the prevision of solvent effects. *Chem. Phys.* **1981**, *55*, 117−129.
(45) Miertuš, S.; Tomasi, J. Approximate evaluations of the electrostatic free energy and internal energy changes in solution processes. *Chem. Phys.* **1982**, *65*, 239−245.
(46) Pascual-ahuir, J. L.; Silla, E.; Tuñon, I. GEPOL: An improved description of molecular surfaces. III. A new algorithm for the computation of a solvent-excluding surface. *J. Comput. Chem.* **1994**, *15*, 1127−1138.
(47) Frisch, M. J.; Trucks, G. W.; Schlegel, H. B.; Scuseria, G. E.; Robb, M. A.; Cheeseman, J. R.; Scalmani, G.; Barone, V.; Mennucci, B.; Petersson, G. A.; Nakatsuji, H.; Caricato, M.; Li, X.; Hratchian, H. P.; Izmaylov, A. F.; Bloino, J.; Zheng, G.; Sonnenberg, J. L.; Hada, M.; Ehara, M.; Toyota, K.; Fukuda, R.; Hasegawa, J.; Ishida, M.; Nakajima, T.; Honda, Y.; Kitao, O.; Nakai, H.; Vreven, T.; Montgomery, J. A., Jr.; Peralta, J. E.; Ogliaro, F.; Bearpark, M.; Heyd, J. J.; Brothers, E.; Kudin, K. N.; Staroverov, V. N.; Kobayashi, R.; Normand, J.; Raghavachari, K.; Rendell, A.; Burant, J. C.; Iyengar, S. S.; Tomasi, J.; Cossi, M.; Rega, N.; Millam, J. M.; Klene, M.; Knox, J. E.; Cross, J. B.; Bakken, V.; Adamo, C.; Jaramillo, J.; Gomperts, R.; Stratmann, R. E.; Yazyev, O.; Austin, A. J.; Cammi, R.; Pomelli, C.; Ochterski, J. W.; Martin, R. L.; Morokuma, K.; Zakrzewski, V. G.; Voth, G. A.; Salvador, P.; Dannenberg, J. J.; Dapprich, S.; Daniels, A. D.; Farkas, O.; Foresman, J. B.; Ortiz, J. V.; Cioslowski, J.; Fox, D. J. *Gaussian 09, Revision D.01*; Gaussian, Inc., Wallingford, CT, 2016.
(48) Francl, M. M.; Pietro, W. J.; Hehre, W. J.; Binkley, J. S.; Gordon, M. S.; DeFrees, D. J.; Pople, J. A. Self-consistent molecular orbital methods. XXIII. A polarization-type basis set for second-row elements. *J. Chem. Phys.* **1982**, *77*, 3654−3665.
(49) Kinart, C. M.; Kinart, W. J.; Kolasiński, A.; Cwiklinska, A.; Dzikowski, T. Studies on Associated Solutions. Part II. Physicochemical Properties of Acetonitrile-Propan-2-ol Mixtures. *Phys. Chem. Liq.* **2000**, *38*, 695−704.
(50) van Meurs, N.; Somsen, G. Excess and apparent molar volumes of mixtures of water and acetonitrile between 0 and 25°C. *J. Solution Chem.* **1993**, *22*, 427−436.
(51) Lata, S.; Singh, K. C.; Ahlawat, S. A study of dielectric properties and refractive indices of aniline + benzene, + toluene, + o-xylene, and + p-xylene at 298.15 K. *J. Mol. Liq.* **2009**, *147*, 191−197.
(52) Maryott, A. A.; Smith, E. R. Table of dielectric constants of pure liquids.*National Bureau of Standards, Circular 514. US Government Printing Office*; **1951**.
(53) Adkins, H.; Broderick, A. E. Hemiacetal formation and the refractive indices and densities of mixtures of certain alcohols and aldehydes. *J. Am. Chem. Soc.* **1928**, *50*, 499−503.
(54) Malek, N. I.; Ijardar, S. P.; Oswal, S. B. Volumetric and acoustic properties of binary mixtures of cyclohexane + benzene and + benzaldehyde at (293.15−323.15) K. *Thermochim. Acta* **2012**, *539*, 71−83.
(55) Kamble, S. P.; Sudake, Y. S.; Patil, S. S.; Khirade, P. W.; Mehrotra, S. C. Solute−Solvent Interaction of Benzene with Acetic Acid at Different Temperatures. *J. Solution Chem.* **2014**, *43*, 1830−1843.

https://doi.org/10.1021/acs.jced.3c00532
J. Chem. Eng. Data 2024, 69, 3573−3583

(56) Aralaguppi, M. I.; Jadar, C. V.; Aminabhavi, T. M. Density, Refractive Index, Viscosity, and Speed of Sound in Binary Mixtures of Cyclohexanone with Benzene, Methylbenzene, 1,4-Dimethylbenzene, 1,3,5-Trimethylbenzene, and Methoxybenzene in the Temperature Interval (298.15 to 308.15) K. *J. Chem. Eng. Data* **1999**, *44*, 446−450.
(57) Ortega, J. Densities and refractive indices of pure alcohols as a function of temperature. *J. Chem. Eng. Data* **1982**, *27*, 312−317.
(58) Ghanadzadeh Gilani, A.; Ghanadzadeh, H.; Bahrpaima, K.; Ranjkesh, A. Dielectric properties of binary mixtures of three butanediols with 1,4-dioxane and 2-ethyl-1-hexanol at T = 298.2 K. *J. Chem. Thermodyn.* **2010**, *42*, 967−972.
(59) Knežević-Stevanović, A. B.; Šerbanović, S. P.; Djordjević, B. D.; Grozdanić, D. K.; Smiljanić, J. D.; Kijevčanin, M. L. Experimental determination and modeling of densities and refractive indices of the binary mixtures of dimethylphthalate (or dimethyladipate) + 1-butanol, or + 2-butanol, or + 2-butanone at T = (288.15−323.15) K. *Thermochim. Acta* **2012**, *533*, 28−38.
(60) Kinart, C. M.; Kinart, W. J.; Chęcińska-Majak, D.; Ćwiklińska, A. Refractive Properties of Binary Mixtures Containing 2-Methoxyethanol and n-Butylamine, Isobutylamine, sec-Butylamine and tert-Butylamine. *Phys. Chem. Liq.* **2003**, *41*, 383−389.
(61) Yaws, C. L. *The Yaws Handbook of Physical Properties for Hydrocarbons and Chemicals*; Elsevier Inc., 2015.
(62) Khasanshin, T. S.; Samuilov, V. S.; Shchamialiou, A. P.; Mosbakh, F. M.; Dragoescu, D.; Sirbu, F. Liquid density measurements of cumene, tert-butylbenzene, and hexadecane over wide ranges of temperature and pressure. *Fluid Phase Equilib.* **2018**, *463*, 121−127.
(63) Ghanadzadeh Gilani, A.; Paktinat, N.; Moghadam, M. Relative permittivity data of binary mixtures containing 2-butanol, 2-butanone, and cyclohexane. *J. Chem. Thermodyn.* **2011**, *43*, 569−575.
(64) Jadżyn, J.; Świergiel, J. Odd−Even Effects in the Static Dielectric Permittivity of a Homologous Series of Liquid Cycloalkanones, (CH2)n-1C=O, n = 4 to 8. *J. Chem. Eng. Data* **2011**, *56*, 4715−4719.
(65) Iloukhani, H.; Rakhshi, M. Excess molar volumes, viscosities, and refractive indices for binary and ternary mixtures of {cyclohexanone (1) + N,N-dimethylacetamide (2) + N,N-diethylethanolamine (3)} at (298.15, 308.15, and 318.15) K. *J. Mol. Liq.* **2009**, *149*, 86−95.
(66) Sastry, N. V.; Valand, M. K. Dielectric constants, refractive indexes and polarizations for 1-Alcohol + Heptane mixtures at 298.15 and 308.15 K. *Bunsenges. Phys. Chem.* **1997**, *101*, 243−250.
(67) Nath, J.; Narain, B. Binary systems of tetrachloroethylene with benzene, toluene, p-xylene, carbon tetrachloride, and cyclohexane. 1. Ultrasonic velocities and adiabatic compressibilities at 293.15 and 303.15 K, dielectric constants at 298.15 and 308.15 K, and refractive indexes at 298.15 K. *J. Chem. Eng. Data* **1982**, *27*, 308−312.
(68) Alonso, V.; González, J. A.; García de la Fuente, I.; Cobos, J. C. Dielectric and refractive index measurements for the systems 1-pentanol + octane, or + dibutyl ether or for dibutyl ether + octane at different temperatures. *Thermochim. Acta* **2012**, *543*, 246−253.
(69) Lago, A.; Rivas, M. A.; Legido, J.; Iglesias, T. P. Study of static permittivity and density of the systems {(n-nonane + monoglyme or diglyme)} at various temperatures. *J. Chem. Thermodyn.* **2009**, *41*, 257−264.
(70) Fu, Y.; Meng, X.; Liang, X.; Wu, J. Density and Viscosity Measurements of 1-Dodecanol and 1,12-Dodecanediol at Temperatures of up to 573.15 K and Pressures of up to 10 MPa. *J. Chem. Eng. Data* **2021**, *66*, 712−721.
(71) Aparicio, S.; Halajian, S.; Alcalde, R.; García, B.; Leal, J. M. Liquid structure of ethyl lactate, pure and water mixed, as seen by dielectric spectroscopy, solvatochromic and thermophysical studies. *Chem. Phys. Lett.* **2008**, *454*, 49−55.
(72) Cepeda, E. A.; Urbano, C. Isobaric Vapor Liquid Equilibrium of 3-Methyl-1-butanol + Ethyl Lactate and 1-Pentanol + Ethyl Lactate at (13.0 and 101.3) kPa. *J. Chem. Eng. Data* **2011**, *56*, 2602−2607.
(73) Sengwa, R. J.; Khatri, V.; Sankhla, S. Dielectric properties and hydrogen bonding interaction behaviour in binary mixtures of glycerol with amides and amines. *Fluid Phase Equilib.* **2008**, *266*, 54−58.
(74) Kijevčanin, M. L.; Živković, E. M.; Djordjević, B. D.; Radović, I. R.; Jovanović, J.; Šerbanović, S. P. Experimental determination and modeling of excess molar volumes, viscosities and refractive indices of the binary systems (pyridine + 1-propanol, + 1,2-propanediol, + 1,3-propanediol, and + glycerol). New UNIFAC-VISCO parameters determination. *J. Chem. Thermodyn.* **2013**, *56*, 49−56.
(75) Grove, E. L.; Walden, G. E. Variation of Dielectric Constant with Temperature for Some Five- and Six-Carbon Ketones. *J. Chem. Eng. Data* **1965**, *10*, 98−100.
(76) Malhotra, R.; Woolf, L. A. Volumetric measurements of liquid pentan-2-one, hexan-2-one, and 4-methylpentan-2-one at temperatures from 278.15 to 338.13 K and pressures in the range from 0.1 to 386 MPa. *J. Chem. Thermodyn.* **1996**, *28*, 1411−1421.
(77) Leiva, L. C.; Jorge, N. L.; Romero, J. M.; Cafferata, L. F. R.; Vara, M. E. G. Kinetics and mechanism of the thermal decomposition reaction of acetone cyclic diperoxide in methyl tert-butyl ether solution. *Int. J. Chem. Kinet.* **2004**, *36*, 302−307.
(78) Rodrıguez, A.; Canosa, J.; Tojo, J. Physical properties of binary mixtures of (t-butyl methyl ether + alcohols) from T = 288.15 K to T = 298.15 K. *J. Chem. Thermodyn.* **1999**, *31*, 1009−1023.
(79) Awwad, A. M.; Al-Dujaili, A. H.; Syriagh, S. R. Dielectric studies of binary mixtures of N-formylmorpholine and an aromatic hydrocarbon. Comparison with theory. *J. Mol. Liq.* **2002**, *100*, 129−141.
(80) Heitele, H.; Pöllinger, F.; Weeren, S.; Michel-Beyerle, M. E. Influence of solvent polarity on intramolecular electron transfer. A consistency test of free energies of reaction and solvent reorganization with experimental rates. *Chem. Phys.* **1990**, *143*, 325−332.
(81) Solimo, H. N.; Martinez, H. E.; Riggio, R. Liquid-liquid extraction of ethanol from aqueous solutions with amyl acetate, benzyl alcohol, and methyl isobutyl ketone at 298.15 K. *J. Chem. Eng. Data* **1989**, *34*, 176−179.
(82) Gardas, R. L.; Johnson, I.; Vaz, D. M. D.; Fonseca, I. M. A.; Ferreira, A. G. M. PVT Property Measurements for Some Aliphatic Esters from (298 to 393) K and up to 35 MPa. *J. Chem. Eng. Data* **2007**, *52*, 737−751.
(83) Cominges, B.E.d.; Pineiro, M. M.; Mascato, E.; Mosteiro, L.; Iglesias, T. P.; Legido, J. L. Relative permittivities of binary mixtures of 1-butanol + n-alkane AT 298.15 k. *J. Therm. Anal. Calorim.* **2003**, *72*, 129−133.
(84) Benito, J.; Guerrero, H.; Artigas, H.; López, M. C.; Lafuente, C. Refractive indices and static permittivities of systems containing n-hexane or n-heptane and isomeric chlorobutanes. *J. Chem. Thermodyn.* **2015**, *86*, 162−167.
(85) Toscani, S.; Figuière, P.; Szwarc, H. A magnetic-suspension apparatus to measure densities of liquids as a function of temperature at pressures up to 100 MPa Application to n-heptane. *J. Chem. Thermodyn.* **1989**, *21*, 1263−1277.
(86) Pereira, S. M.; Rivas, M. A.; Real, J. N.; Legido, J. L.; Iglesias, T. P. Densities, Speeds of Sound, and Refractive Indices of the Mixture Nonane + Triethylene Glycol Dimethyl Ether at 288.15 K, 293.15, K, 298.15, K, and 308.15 K. *J. Chem. Eng. Data* **2002**, *47*, 919−922.
(87) Anderson, J.; Berthod, A.; Pino, V.; Stalcup, A. M. *Analytical Separation Science*; John Wiley & Sons, 2015.
(88) Navarro, P.; Larriba, M.; García, S.; García, J.; Rodríguez, F. Physical Properties of Binary and Ternary Mixtures of 2-Propanol, Water, and 1-Butyl-3-methylimidazolium Tetrafluoroborate Ionic Liquid. *J. Chem. Eng. Data* **2012**, *57*, 1165−1174.
(89) Murakami, S.; Fujishiro, R. The Heats of Mixing for Binary Mixtures. III. The Intermolecular Energy of Hydrogen Bonding between Alcohol and Several Other Polar Molecules. *Bull. Chem. Soc. Jpn.* **1966**, *39*, 720−725.
(90) Vercher, E.; Llopis, F. J.; González-Alfaro, M. V.; Martínez-Andreu, A. Density, Speed of Sound, and Refractive Index of 1-Ethyl-3-methylimidazolium Trifluoromethanesulfonate with Acetone, Methyl Acetate, and Ethyl Acetate at Temperatures from (278.15 to 328.15) K. *J. Chem. Eng. Data* **2010**, *55*, 1377−1388.
(91) Otín, S.; Fernández, J.; Embid, J. M.; Velasco, I.; Losa, C. G. Thermodynamic and Dielectric Properties of Binary Polar + Non-Polar Mixtures I. Static Dielectric Constants and Excess Molar Enthalpies of n-Alkylamine + n-Dodecane Systems. *Bunsenges. Phys. Chem.* **1986**, *90*, 1179−1183.

https://doi.org/10.1021/acs.jced.3c00532
J. Chem. Eng. Data 2024, 69, 3573−3583

(92) Pal, A.; Kumar, H.; Sharma, S.; Maan, R.; Sharma, H. K. Mixing Properties for Binary Liquid Mixtures of Methyl tert-Butyl Ether with Propylamine and Dipropylamine at Temperatures from (288.15 to 308.15) K. *J. Chem. Eng. Data* **2010**, *55*, 1424−1429.
(93) Lechner, M. D. *Static Dielectric Constants of Pure Liquids and Binary Liquid Mixtures: Supplement to IV/6*; Springer Berlin, Heidelberg, 2008.
(94) Steele, W. V.; Archer, D. G.; Chirico, R. D.; Collier, W. B.; Hossenlopp, I. A.; Nguyen, A.; Smith, N. K.; Gammon, B. E. The thermodynamic properties of quinoline and isoquinoline. *J. Chem. Thermodyn.* **1988**, *20*, 1233−1264.
(95) Vahidi, M.; Moshtari, B. Dielectric data, densities, refractive indices, and their deviations of the binary mixtures of N-methyldiethanolamine with sulfolane at temperatures 293.15−328.15 K and atmospheric pressure. *Thermochim. Acta* **2013**, *551*, 1−6.
(96) Ritzoulis, G.; Papadopoulos, N.; Jannakoudakis, D. Densities, viscosities, and dielectric constants of acetonitrile + toluene at 15, 25, and 35 °C. *J. Chem. Eng. Data* **1986**, *31*, 146−148.
(97) Singh, R. P.; Sinha, C. P. Viscosities and activation energies of viscous flow of the ternary mixtures of toluene, chlorobenzene, 1-hexanol, and benzyl alcohol. *J. Chem. Eng. Data* **1985**, *30*, 470−474.
(98) Owen, B. B.; Miller, R. C.; Milner, C. E.; Cogan, H. L. The dielectric constant of water as a function of temperature and pressure. *J. Phys. Chem.* **1961**, *65*, 2065−2070.
(99) Hale, G. M.; Querry, M. R. Optical Constants of Water in the 200-nm to 200-μm Wavelength Region. *Appl. Opt.* **1973**, *12*, 555−563.
(100) Tanaka, M.; Girard, G.; Davis, R.; Peuto, A.; Bignell, N. Recommended table for the density of water between 0 and 40 °C based on recent experimental reports. *Metrologia* **2001**, *38*, 301−309.
(101) Weinhold, F.; Landis, C. R. *Valency and Bonding: A Natural Bond Orbital Donor-Acceptor Perspective*; Cambridge University Press, 2005. DOI: 10.1017/CBO9780511614569.
(102) Bondi, A. van der Waals Volumes and Radii. *J. Phys. Chem.* **1964**, *68*, 441−451.
(103) Velho, P.; Liang, X.; Macedo, E. A.; Gómez, E.; Kontogeorgis, G. M. Towards a predictive Cubic Plus Association equation of state. *Fluid Phase Equilib.* **2021**, *540*, 113045.

https://doi.org/10.1021/acs.jced.3c00532
J. Chem. Eng. Data 2024, 69, 3573−3583